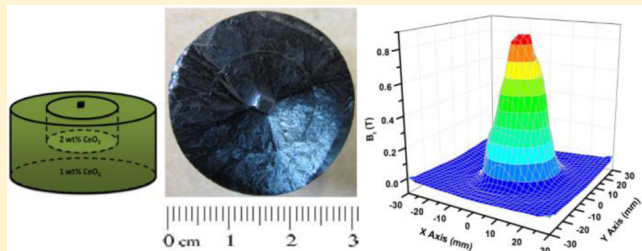


Processing and Properties of Bulk Y–Ba–Cu–O Superconductors Fabricated by Top Seeded Melt Growth from Precursor Pellets Containing a Graded CeO₂ Composition

Wei Zhai,* Yunhua Shi, John H. Durrell, Anthony R. Dennis, Zhiwei Zhang, and David A. Cardwell

Department of Engineering, University of Cambridge, Trumpington Street, Cambridge, CB2 1PZ, U.K.

ABSTRACT: The existence of a zone containing a low concentration of Y₂BaCuO₅ (Y-211) phase particles in the vicinity of the seed in single grain, bulk Y–Ba–Cu–O (YBCO) superconductors fabricated by the top seeded melt growth (TSMG) technique has been reported, suggesting the presence of low intrinsic magnetic flux pinning, and hence reduced trapped field, in this region of the sample. The possibility of introducing additional pinning centers in the vicinity of the seed in single grain YBCO, therefore, may be effective in improving the applied magnetic properties of these technologically important materials. Single grain, bulk YBCO superconductors fabricated from precursor pellets containing a graded CeO₂ composition have been prepared corresponding to a secondary phase content of 2 wt % CeO₂ beneath the seed and 1 wt % CeO₂ at the outer, “U” shape cross-section, of the sample. The resulting graded single grain YBCO superconductors exhibit enhanced trapped field compared to standard YBCO superconductors fabricated by TSMG from precursor pellets containing purely 1 wt % CeO₂. The influence of CeO₂ content on the microstructure, growth process, and superconducting properties of bulk, single grain YBCO superconductors fabricated by TSMG has been investigated and used to explain the increased trapped field ability of the graded composition.



1. INTRODUCTION

Bulk, single grain Y–Ba–Cu–O (YBCO) superconductors have a significant potential for high field, permanent magnet applications¹ such as flywheel energy storage systems² and magnetic bearings³ due to their ability to trap large magnetic fields at the boiling point of liquid nitrogen (77 K).⁴ The field trapping ability of these technologically important materials depends critically on the ability to engineer a rather uniformly distributed high critical current density (J_c) throughout the sample in the presence of an applied magnetic field (B).⁵ From a materials processing point of view, it is the control of a uniform distribution of flux pinning centers within the YBCO matrix that is critical to ensure a uniform distribution of high J_c throughout the bulk sample and therefore to yield a high trapped field.

The top seeded melt growth (TSMG) technique has been established over the past 20 years as an effective way of growing bulk, single grain YBCO superconductors.⁶ In this process, an excess of small Y₂BaCuO₅ (Y-211) phase particles is usually added to the precursor powder to enhance the concentration of unreacted, undissolved Y-211 inclusions in the superconducting YBa₂Cu₃O_{7-δ} (Y-123) phase matrix within the fully processed bulk YBCO superconductor, which, in turn, create Y-211/Y-123 interfaces that can act as effective flux pinning centers to improve J_c of the single grain.⁷ However, the presence of a zone of low-Y-211 content, and therefore a region of low pinning center density, in the vicinity of the seed crystal in single grain YBCO has been discovered and reported by several groups.⁸⁻¹¹

This zone of low pinning center density contributes to an inhomogeneous distribution of J_c and therefore to a reduced value of trapped field value.^{12,13} As a result, it is important to introduce additional pinning centers in the region of the single grain in the vicinity of the seed in order to improve the field trapping ability of bulk YBCO superconductors for practical applications.¹⁴

It has been reported that CeO₂ particles can react with Y-211 particles prior to the melting process to produce BaCeO₃ particles, which can form effective flux pinning centers.¹⁵⁻¹⁸ Moreover, CeO₂ powders are usually added to the precursor powders in the TSMG process as an effective way of reducing the size of Y-211 inclusions, and therefore to increase J_c throughout the whole sample.^{15,16} Several groups have also observed the “peak effect” in the magnetization curve of bulk YBCO superconductors processed with CeO₂ additions.¹⁹⁻²² This suggests that the introduction of additional CeO₂ in the vicinity of the seed during the melt process has significant potential for overcoming the problem of a low pinning centers density at the center of YBCO superconductors grown using the TSMG process.⁸

We have reported previously the successful fabrication of bulk, single grain YBCO superconductors from precursor pellets containing a graded Y-211 precursor composition using

Received: November 26, 2014

Revised: December 23, 2014

Published: January 8, 2015

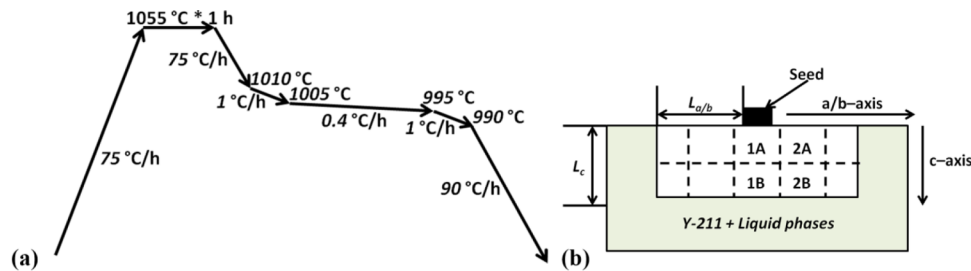


Figure 1. (a) Temperature profile used to fabricate single grain YBCO samples #1W and #2W with a diameter of ~14 mm. (b) Schematic cross-section of a YBCO single grain, illustrating the position of the specimens for the measurement of T_c and J_c .

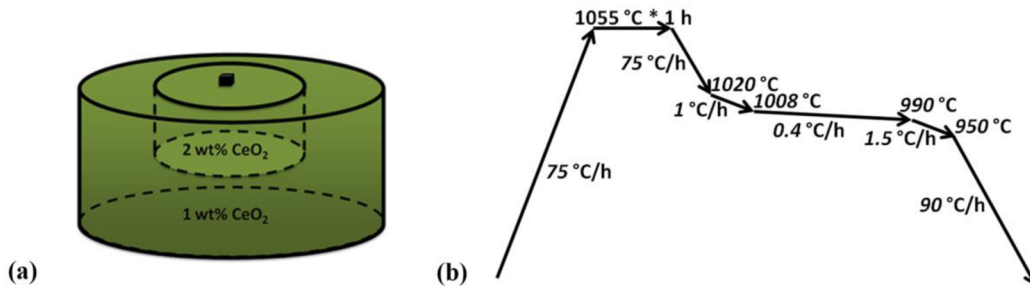


Figure 2. (a) Schematic diagram of a graded-CeO₂ single grain sample processed from precursor powders containing 2 and 1 wt % CeO₂ arranged in a 'U'-shape cross-sectional geometry. (b) The temperature profile used to fabricate YBCO superconductors of diameter of ~20 mm.

the TSMG process.²³ In this paper, and based on this previous work, we report the fabrication and characterization of bulk YBCO superconductors from precursor pellets containing a graded CeO₂ composition, consisting specifically of 2 wt % CeO₂ + 70 wt % Y-123 + 30 wt % Y-211 in the vicinity of the seed and 1 wt % CeO₂ at the outer parts of the sample. Bulk, ungraded YBCO superconductors fabricated from precursor powders containing only 1 and 2 wt % CeO₂, respectively, were also grown by TSMG for purposes of comparison. The influence of CeO₂ content on the superconducting properties, microstructure, and growth process of bulk YBCO superconductors was investigated initially as part of this study. The growth morphology and superconducting properties of the samples, in particular, have been studied and compared. The trapped field was determined by a rotating Hall Probe arrangement, and the critical temperature and critical current density were characterized using a SQUID magnetometer. Finally, we investigate whether the addition of precursor powder containing excess CeO₂ to the center of the sample is effective in improving the field trapping ability of bulk YBCO superconductors for high field, practical applications.

2. EXPERIMENTAL PROCEDURES

2.1. Preparation of Precursor Powders. Precursor powders were prepared by mixing thoroughly commercially available Y-123, Y-211, and CeO₂ powders using a motorized pestle and mortar. The Y-123 and Y-211 powders were supplied by the Toshima Manufacturing Co. Ltd. and had a purity of 99.9% and particle size of 2–3 μm and approximately 1 μm , respectively. The CeO₂ powders were supplied by Alfa Aesar and had a purity of 99.9%. Two types of precursor powders were prepared by mixing the Y-123, Y-211, and CeO₂ powders in different weight ratios, and labeled based on their CeO₂ content. The 1 wt % CeO₂ precursor powders were prepared with a component weight ratio of Y-123/Y-211/CeO₂ of 70:30:1 and the 2 wt % CeO₂ precursor powders with a ratio of 70:30:2.

2.2. Fabrication of Single Grain YBCO Superconductors. Two types of ungraded green pellets were prepared initially from precursor powders containing 1 and 2 wt % CeO₂ by pressing uniaxially the

relevant powders into cylindrical pellets of diameter ~16.0 mm and thickness ~7 mm under a load of between 2 and 3 tons. An NdBCO single crystal seed, cleaved along the *a/b* plane, was placed at the center of the upper surface of each green pellet. The green pellets were then placed in the same chamber of a four-chamber furnace and processed by TSMG using the temperature profile shown in Figure 1a. The as-grown samples were annealed at 450 °C for 7 days in flowing oxygen to transform fully the nonsuperconducting tetragonal Y-123 phase to the superconducting orthorhombic phase. The as-grown YBCO samples were labeled as #1W and #2W for the precursor compositions containing 1 wt % CeO₂ and 2 wt % CeO₂ precursor powders, respectively. The diameter and height of the as-grown #1W and #2W YBCO superconductors were approximately 14 mm and 6 mm.

Precursor pellets containing a graded CeO₂ composition were prepared by arranging two types of precursor powders in a U-shape geometry through the cylindrical pellet cross-section, with the 2 wt % CeO₂ precursor powders at the center and the 1 wt % CeO₂ powders in the outer U-layer of the samples, as shown schematically in Figure 2a. The graded-CeO₂ precursor pellets had an overall weight of ~20 g, a diameter of ~25 mm, and a thickness of ~12 mm. The ungraded precursor pellets containing only 1 wt % CeO₂ and 2 wt % CeO₂ had the same volume as the graded-CeO₂ precursor pellet to enable meaningful comparison. The same TSMG and annealing processes were used to fabricate single grain bulk YBCO superconductors from both graded and ungraded precursor pellets, but with an adjusted temperature profile, as shown in Figure 2b. Three graded-CeO₂ YBCO superconductors (labeled as #G-1, #G-2, and #G-3), three 1 wt % CeO₂ containing (labeled as #1W-1, #1W-2, and #1W-3), and one 2 wt % CeO₂ containing YBCO superconductors (labeled as #2W-1) were prepared successfully and analyzed as part of this investigation. The diameter and height of the as-grown YBCO superconductors were approximately 20 mm and 9.5 mm, respectively.

2.3. Characterization. Samples #1W and #2W of diameter ≈ 14 mm were cut in half through the position of the seed using a diamond wheel. The exposed cross sections were ground successively using 500, 800, 1000, 1200, 2400 grit SiC paper and polished additionally with 3 and 1 μm diamond spray using only ethanol for lubrication during the polishing process. Backscattered electron scanning electron microscopy (SEM) images at magnification of 50 and 1000 times were taken about 1 mm below the seed of samples #1W and #2W, respectively,

using SEM (SEM S-3400N) to investigate the effect of CeO₂ addition on the microstructure of the single grains.

The effect of CeO₂ addition on the superconducting properties of the single grain samples was investigated by cutting small specimens of size approximately 1.5 mm × 2.0 mm × 1.2 mm from different positions of samples #1W and #2W, as indicated in Figure 1b. These specimens were used to measure the transition temperature (T_c) and the critical current density (J_c) at 77 K at different positions within each parent bulk using a Quantum Design MPMS XL SQUID magnetometer. The temperature dependence of magnetic moment was measured using zero field cooling method under an applied field of 20 Oe for the determination of T_c . For the measurement of the magnetic moment loops, the applied magnetic field was swept from -6 to 6 T and a small scan length (3 cm) selected to ensure reasonable field uniformity. The extended Bean model²⁴ was used to calculate $J_c(B)$ from the measured magnetic moment hysteresis loops.

Three graded-CeO₂ YBCO superconductors, three YBCO superconductors containing 1 wt % CeO₂ and one YBCO superconductor containing 2 wt % CeO₂ with a diameter of ~20 mm were field-cooled to 77 K under an applied external magnetic field of 1.2 T for trapped field measurement. The top surface of each sample was flux mapped using a rotating, linear array of 20 Hall probes positioned ~0.5 mm above the sample surface. The maximum trapped field value was calibration corrected from the data measured by a hand-held Gaussmeter probe using the equation $B_{t,\max} = 0.8586B_{\text{hand}} + 0.0298$, which had been determined from a previous study. The three-dimensional (3D) contour map of the trapped field distribution obtained by this process was adjusted and plotted using Origin software.

3. RESULTS AND DISCUSSION

3.1. Growth Morphology. Figure 3 shows photographs of the top surfaces of samples #1W and #2W, with diameters of

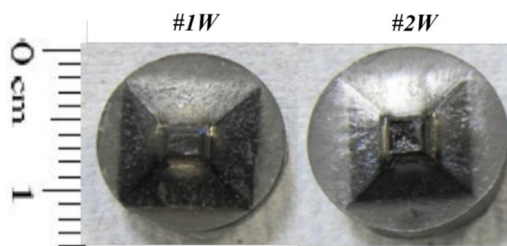
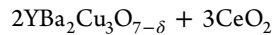
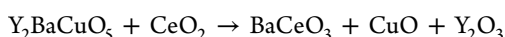


Figure 3. Photographs of the top surfaces of samples #1W and #2W of diameter of ~14 mm.

~14 mm, respectively. It can be seen that both samples were grown epitaxially from the seed into homogeneous single grains with well-defined facet lines and without subgrain formation. This demonstrates clearly that YBCO single grains can be fabricated successfully from precursor powders containing 1 and 2 wt % CeO₂. However, it is noticeable that the facet lines extend to the edge of the #1W YBCO single grain, but terminate approximately 1 mm away from the edge of sample #2W. It may be concluded that the growth rate of the single grain is influenced by the CeO₂ content, since the same temperature profile was used to process both samples, and, from the growth morphology analysis, that the growth rate of the YBCO single grain decreases as the CeO₂ content in the precursor powders increases.

3.2. SEM Examination. Piñol et al.^{15,16} reported that CeO₂ reacts with Y-211 and Y-123 below the Y-123 peritectic decomposition temperature, according to the following reactions:



The reaction product BaCeO₃, which does not react with the melt during the subsequent melt-process,¹⁶ can be recognized readily in the backscattered electron SEM images, since its contrast is significantly greater than that of the Y-211 particles and the Y-123 phase matrix.¹⁶

Backscattered electron SEM images at magnification of 50 and 1000 times were taken about 1 mm below the seed of samples #1W and #2W, respectively, to investigate the effect of CeO₂ addition on the microstructure of the single grains, as shown in Figure 4. The lump of bright-in-contrast particles, in

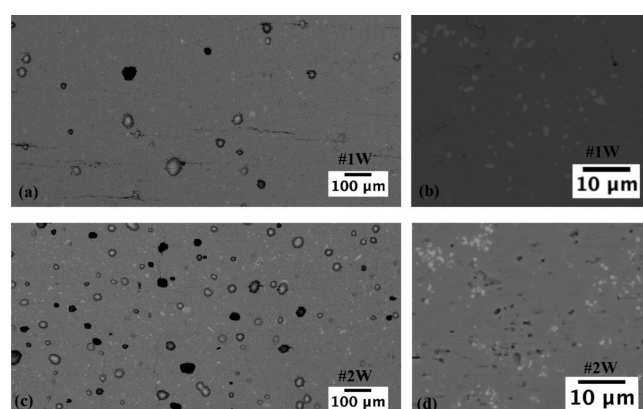


Figure 4. Backscattered electron SEM images showing the microstructures of samples (a) #1W in magnification of 50×, (b) #1W in 1000×, (c) #2W in 50×, and (d) #2W in 1000×.

Figure 4a,c of low magnification images, are BaCeO₃ particles, which are randomly distributed in the Y-123 matrix. It can be seen more clearly from Figure 4b,d of large magnification that BaCeO₃ particles are embedded in the Y-123 matrix, which have a bright-in-contrast and well-defined, faceted shape. It is clear from Figure 4 that the content of BaCeO₃ particles embedded in the samples is greater for sample #2W than for sample #1W, which correlates directly, and perhaps unsurprisingly, with the initial CeO₂ content in the precursor powder.

3.3. Measurements of T_c . Figure 5 shows the results of the measurement of the transition temperature (T_c) ($B = 2$ mT, $B \parallel c$) for samples #1W and #2W at positions 1A and 2A (Figure 1b). It can be seen that the onset T_c for both samples at both positions is consistently around 90 K, and that the T_c of every sample exhibits a relatively sharp transition. Therefore, both samples #1W and #2W were well oxygenated and exhibit good connectivity, which enables effective comparison of their J_c - B properties.

3.4. Estimation of J_c - B at 77 K. Figure 6a-d compares the J_c - B (77 K, $B \parallel c$) curves of samples #1W and #2W at positions 1A, 2A, 1B, and 2B, respectively. The position of each specimen is illustrated schematically in Figure 1b. J_c varies with position within each specimen due directly to the effects of grain misorientation and defects, such as cracks, pores, and impurities. As a result, four specimens at different positions within each sample #1W and #2W were selected and characterized for comparison.

It can be seen from Figure 6a that J_c at position 1A is higher for sample #2W than for sample #1W when the external magnetic field is between 0 T and ~3 T. The rate of decrease of

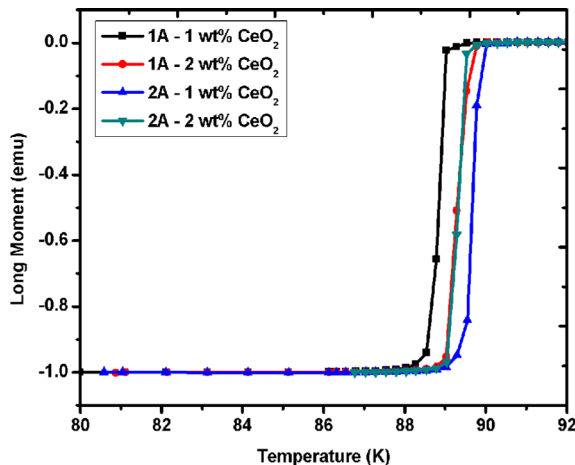


Figure 5. Measurement of T_c for samples #1W and #2W at positions 1A and 2A within the parent single grain.

J_c with increasing B for sample #2W at position 1A decreases significantly, and particularly for fields between ~ 0.5 and ~ 2 T, where a value of around $10\,000$ A/cm 2 is observed. However, the J_c - B curve for sample #1W at the same position within the single grain decreases continuously to about 7500 A/cm 2 as the magnetic field increases to ~ 2 T. The enhanced J_c at higher magnetic field for sample #2W is more pronounced at position 2A, as can be seen from Figure 6b. It is noticeable that the values of J_c of sample #2W at position 2A are almost twice those for sample #1W between ~ 0.5 T and ~ 2 T. Moreover,

the J_c values of sample #2W exhibit an upward trend as the external magnetic field increases in this field region, whereas the values of J_c for sample #1W continue to decrease. Although the difference is not large, the J_c - B curves of sample #2W at position 1B, are still higher than for sample #1W between ~ 0.5 T and ~ 3.5 T (Figure 6c). It is clear that the J_c - B curves for sample #2W are generally higher than those for sample #1W in fields of up to 4 T for position 2B (Figure 6d).

The J_c (B) results are in consistent with the observations reported by several groups that there is “peak effect” in the magnetization curve of bulk YBCO superconductors processed with CeO₂ additions.^{19,20,25,26} The explanations of this phenomenon of enhanced critical current densities at higher magnetic field are either due to oxygenation stoichiometry or Ce substitution. In the former case, it was considered that the Ce additions lead to a denser sample, making oxygenation more difficult, hence the formation of a peak as a function of oxygenation.^{20,26} On the other hand, MaGinn et al.^{19,25} believe that the peak effect is the result of Ce substitution into the Y-123 lattice. In conclusion, it is clear from a comparison of the field-dependent J_c that the single grain YBCO sample grown from precursor pellets containing 2 wt % CeO₂ exhibit enhanced critical current densities than those containing 1 wt % CeO₂. In addition, it is particularly evident that the improvement in critical current density of the sample containing 2 wt % CeO₂ is more significant at higher magnetic field (~ 0.5 T to ~ 2 T).

3.5. Analysis of Trapped Fields. Figure 7 shows photographs of the top surfaces of all the three graded-CeO₂

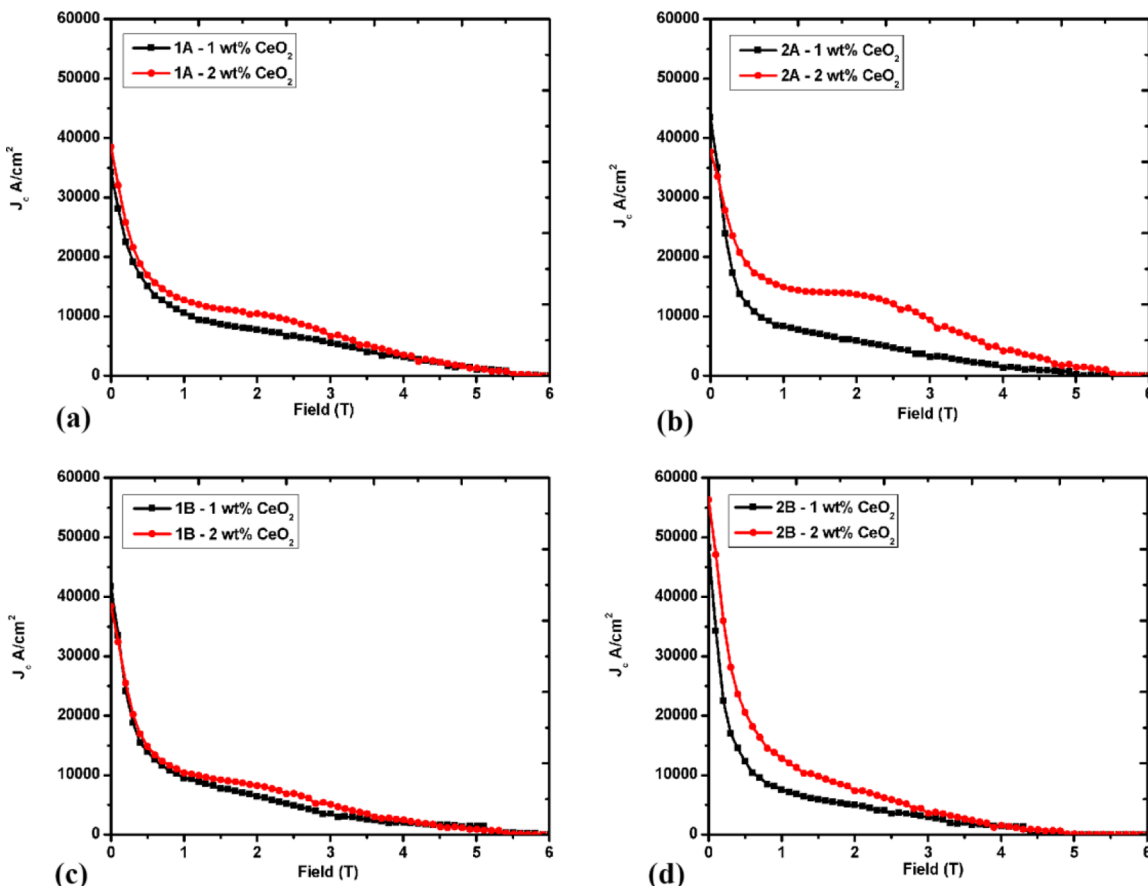


Figure 6. J_c (B) for samples #1W and #2W at 77 K at positions (a) 1A, (b) 2A, (c) 1B, and (d) 2B in the parent single grain.



Figure 7. Photographs of the top surfaces the three graded-CeO₂, the three 1 wt % CeO₂, and one 2 wt % CeO₂ single grain YBCO superconductor with a diameter of ~20 mm prepared as part of this study.

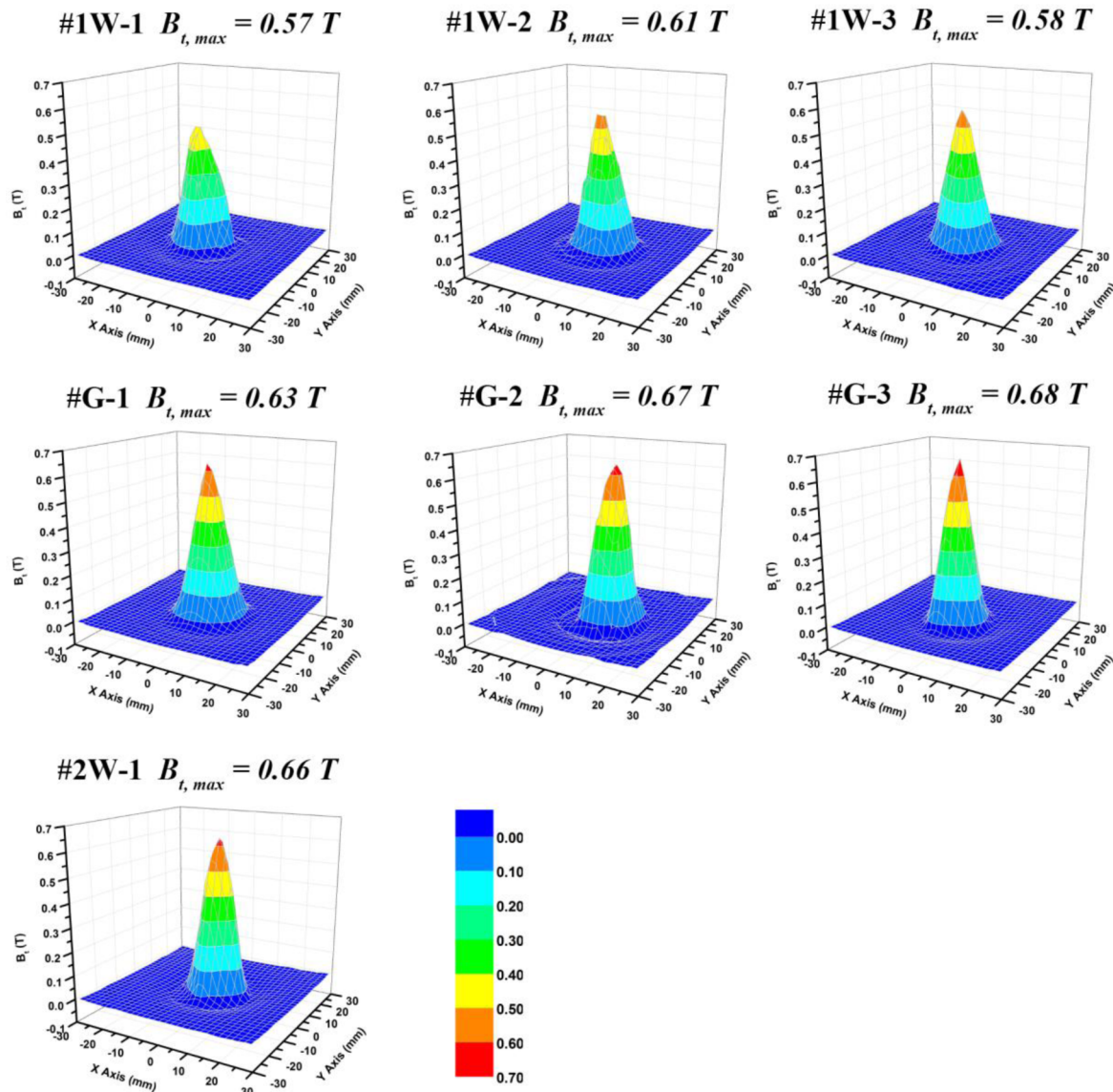


Figure 8. 3D contour maps of the trapped field distributions of the three graded-CeO₂, three 1 wt % CeO₂ and one 2 wt % CeO₂ single grain YBCO superconductor with a diameter of ~20 mm at 77 K.

samples, three samples containing 1 wt % CeO₂ and one sample containing 2 wt % CeO₂, each of which have a diameter of ~20 mm. It can be seen that all seven samples exhibit well-defined, 4-fold growth symmetry, which indicates that each faceted single grain has grown homogeneously.

Figure 8 shows the 3D contour plots of the trapped field distribution of the three graded-CeO₂ samples, three 1 wt % CeO₂ containing and one 2 wt % CeO₂ containing YBCO superconductors (each with a with diameter of ~20 mm) at 77

K. The color contour scale for the trapped field for each sample is the same in the figure. The maximum-trapped field value for each sample is shown above its associated 3D contour image. It is clear from Figure 8 that all seven samples exhibit a single peak in their trapped field distribution profile, which means they are all well oxygenated and are the product of well-aligned, single grain growth. The maximum-trapped field values observed for YBCO superconductors grown from precursor powders containing 1 wt % CeO₂ are 0.57, 0.61, and 0.58 T,

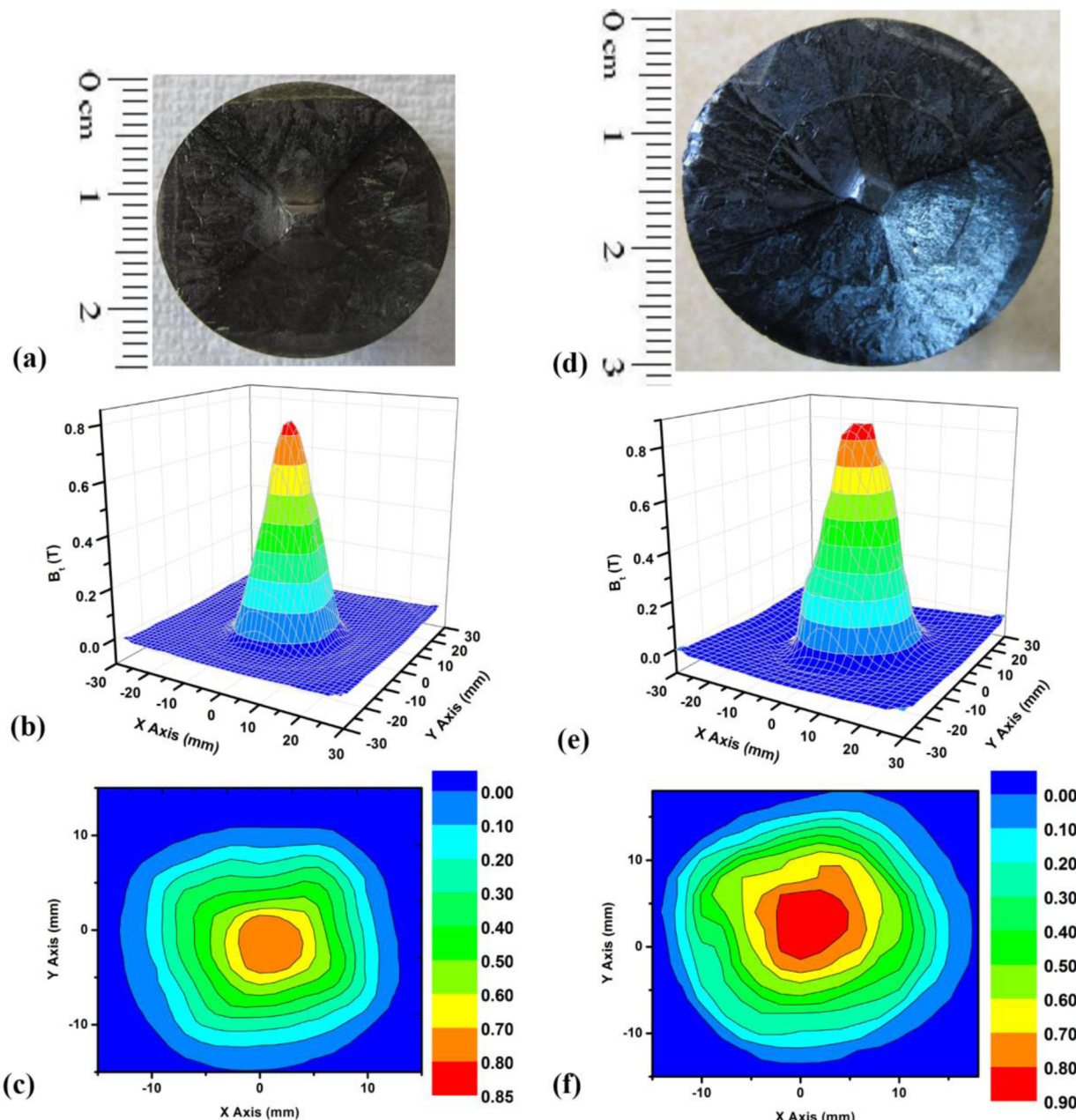


Figure 9. (a) Photograph of the top surface of the graded- CeO_2 YBCO superconductor with a diameter of ~ 25 mm, (b) the 3D contour of the trapped field distribution and (c) the 2D contour map of the trapped field distribution of this sample. (d) Photograph of the top surface of the graded- CeO_2 YBCO superconductor with diameter of ~ 31 mm, (e) the 3D contour of the trapped field distribution, and (f) the 2D contour map of the trapped field distribution of this sample.

respectively. YBCO superconductors grown from graded- CeO_2 precursor pellets show trapped field values higher than the samples containing 1 wt % CeO_2 , which are 0.63, 0.67, and 0.68 T, respectively. Therefore, the graded- CeO_2 YBCO superconductors exhibit higher trapped field values than YBCO superconductors grown from precursor powders containing 1 wt % CeO_2 . The YBCO superconductor grown from precursor powders containing 2 wt % CeO_2 exhibit a maximum trapped field of 0.66 T, which is higher than the YBCO superconductors grown from precursor powders containing 1 wt % CeO_2 , but lies generally within the range of the trapped field values observed for the graded- CeO_2 YBCO superconductor.

From the above analysis, YBCO superconductors with a diameter of ~ 20 mm grown from the graded CeO_2

composition generally exhibit higher values of trapped field than those grown from precursor powders containing 1 wt % CeO_2 . Bulk, graded- CeO_2 YBCO superconductors with a relatively larger diameter of ~ 25 mm and ~ 31 mm were grown subsequently for trapped field analysis, in order to verify the reliability of the graded- CeO_2 TSMG method. Figure 9a–c shows a photograph of the top surface of a bulk YBCO superconductor of diameter ~ 25 mm together with 3D and 2D contour of the associated trapped field distribution. Figure 9d–f shows the corresponding characteristics of the graded bulk YBCO superconductor with diameter of ~ 31 mm. It can be seen from the growth morphology that both graded- CeO_2 samples were grown fully into well-aligned, YBCO single grains. The 3D and 2D contour maps of the trapped field distribution

of both samples exhibit a single peak, which indicates a uniform distribution of trapped field within each sample. The maximum-trapped field value of the graded-CeO₂ YBCO superconductors of diameter ~25 mm is 0.81 T at 77 K, which increases to 0.92 T at 77 K for the sample with a diameter of ~31 mm. This demonstrates clearly that bulk YBCO superconductors with a large diameter can be grown successfully from precursor pellets containing a graded CeO₂ composition by the TSMG technique.

It can be concluded from the trapped field analysis that YBCO superconductors grown from the graded CeO₂ composition exhibit higher values of trapped field than samples grown from precursor powders containing 1 wt % CeO₂. There are two reasons contributing to this phenomenon. First, from the SEM analysis, it can be concluded that the addition of increasing quantities of CeO₂ to the precursor powder generates a greater concentration of BaCeO₃ particles, which can work as pinning centers,^{15–18} in the fully processed sample. Since the YBCO superconductors processed from 1 wt % CeO₂ precursor powders contain a relatively small number of Y-211 particles in the region of the sample in the vicinity of the seed, there are only a limited number of flux pinning centers, as discussed in the Introduction.^{8,10} The addition of 2 wt % CeO₂ to graded-CeO₂ YBCO superconductors could generate additional BaCeO₃ inclusions, and therefore more pinning centers, in the vicinity of the seed than that observed for the samples containing 1 wt % CeO₂. Second, from the J_c analysis, we can conclude that the addition of 2 wt % CeO₂ contributes to an enhanced critical current density at a higher magnetic field (~0.5 T to ~2 T). Since the area beneath the seed corresponds physically to the center of the sample, this area is under the position of the highest value of magnetic field generated by the sample.²⁷ From the trapped field analysis, the center of the graded-CeO₂ YBCO superconductors experiences a magnetic field higher than 0.5 T. Therefore, the $J_c(B)$ values of the graded-CeO₂ YBCO superconductor in the area beneath the seed are higher than the sample containing 1 wt % CeO₂ due to the enhanced $J_c(B)$ effect.²⁷ In conclusion, the peak value of the trapped field depends usually on sample size and $J_c(B)$.⁶ The graded-CeO₂ YBCO superconductors have more BaCeO₃ pinning centers and exhibit higher values of $J_c(B)$ in the area beneath the seed than the samples containing 1 wt % CeO₂, which contribute directly to the observed higher trapped field of the graded-CeO₂ YBCO superconductors.

The YBCO superconductors containing 2 wt % of CeO₂ also exhibit higher trapped fields than the samples containing 1 wt % CeO₂. However, in this research, only one out of five sample containing 2 wt % CeO₂ YBCO with a diameter of ~20 mm, were grown successfully. The low success rate of the growth of the YBCO superconductors containing 2 wt % CeO₂ of diameter of ~20 mm is direct evidence of the reduced growth rate due to the addition of 2 wt % CeO₂. YBCO superconductors grown from the graded-CeO₂ precursor powders, on the other hand, were processed with a much greater success rate. Graded-CeO₂ YBCO superconductors with larger diameters of ~25 mm and ~31 mm can also be grown successfully, and also exhibit relatively high trapped fields. Therefore, the graded-CeO₂ bulk YBCO superconductors exhibit both high trapping magnetic field ability and can be grown with a relatively high success rate, which is significant for the development of practical applications of these materials.

4. CONCLUSION

We have succeeded in enhancing the field trapping ability of bulk, single grain YBCO superconductors fabricated by the top seeded melt growth technique by employing a graded CeO₂ composition in the precursor pellet. Graded-CeO₂ YBCO superconductors, which contain 2 wt % CeO₂ at the center and 1 wt % CeO₂ at the outer parts of the sample, were fabricated successfully as part of this study, overcoming the difficulties of reduced growth rate associated with a higher CeO₂ concentration at the center of the sample. The number of BaCeO₃ pinning centers generated in the superconducting Y-123 phase matrix was increased in the single grain YBCO fabricated from precursor powders containing 2 wt % CeO₂. As a result, enhanced values of J_c , and particularly at a higher magnetic field, have been observed in the $J_c(B)$ curves of these single grain superconductors. Single grain samples grown from graded-CeO₂ precursor pellets exhibit trapped field values (0.63 T, 0.67 and 0.68 T) that are significantly higher than those of the single grain samples containing 1 wt % CeO₂ (0.57, 0.61, and 0.58 T). Bulk, YBCO superconductors containing 2 wt % CeO₂ exhibit trapped fields as high as the graded-CeO₂ YBCO superconductors, although these samples cannot be melt processed reliably. Large, bulk graded-CeO₂ YBCO superconductors with diameters of ~25 mm and ~31 mm have been fabricated successfully based on the results of this study and observed to exhibit high trapped fields (0.81 and 0.92 T at 77 K). It is clear from this investigation that graded-CeO₂ single grain YBCO superconductors have the advantages of both exhibiting high values of trapped field and the potential to be melt processed reliably with a high rate of success. Therefore, we have demonstrated the graded-CeO₂ TSMG process to be effective in growing single grain YBCO superconductors with improved field trapping ability, which is potentially significant in the development of bulk YBCO superconductors for practical applications.

■ AUTHOR INFORMATION

Corresponding Author

*Tel: +44 1223 32831. E-mail: wz253@cam.ac.uk.

Notes

The authors declare no competing financial interest.

■ ACKNOWLEDGMENTS

This work was supported by the Engineering and Physical Sciences Research Council, EPSRC, [Grant Number EP/K02910X/1]. W.Z. would like to acknowledge financial support from the China Scholarship Council and the Cambridge Commonwealth, European and International Trust.

■ REFERENCES

- (1) Campbell, A. M.; Cardwell, D. A. *Cryogenics* **1997**, *37*, 567–575.
- (2) Miyagawa, Y.; Kameno, H.; Takahata, R.; Ueyama, H. *IEEE Trans. Appl. Supercond.* **1999**, *9*, 996–999.
- (3) Hull, J. *Supercond. Sci. Technol.* **2000**, *13*, R1–R15.
- (4) Durrell, J. H.; Dennis, A. R.; Jaroszynski, J.; Ainslie, M. D.; Palmer, K. G. B.; Shi, Y.; Campbell, A. M.; Hull, J.; Strasik, M.; Hellstrom, E.; Cardwell, D. A. *Supercond. Sci. Technol.* **2014**, *27*, 082001.
- (5) Cloots, R.; Koutzarova, T.; Mathieu, J.-P.; Ausloos, M. *Supercond. Sci. Technol.* **2005**, *18*, R9–R23.
- (6) Cardwell, D. *Mater. Sci. Eng., B* **1998**, *53*, 1–10.
- (7) Murakami, M.; Yamaguchi, K.; Fujimoto, H.; Nakamura, N.; Taguchi, T.; Koshizuka, N.; Tanaka, S. *Cryogenics* **1992**, *32*, 930–935.

- (8) Zhai, W.; Shi, Y.; Durrell, J. H.; Dennis, A. R.; Cardwell, D. A. *Cryst. Growth Des.* **2014**, *14*, 6367–6375.
- (9) Delamare, M. P.; Walter, H.; Bringmann, B.; Leenders, A.; Freyhardt, H. C. *Phys. C Supercond.* **1999**, *323*, 107–114.
- (10) Endo, A.; Chauhan, H. S.; Egi, T.; Shiohara, Y. *J. Mater. Sci.* **1996**, *11*, 795–803.
- (11) Chow, J. C. L.; Lo, W.; Leung, H.-T.; Dewhurst, C. D.; Cardwell, D. A. *Mater. Sci. Eng., B* **1998**, *53*, 79–85.
- (12) Desgardin, G.; Monot, I.; Raveau, B. *Supercond. Sci. Technol.* **1999**, *12*, R115–R133.
- (13) Lee, D. F.; Selvamanickam, V.; Salama, K. *Phys. C Supercond.* **1992**, *202*, 83–96.
- (14) Murakami, M. *Mod. Phys. Lett. B* **1990**, *04*, 163.
- (15) Piñol, S.; Sandiumenge, F.; Martínez, B.; Gomis, V.; Fontcuberta, J.; Obradors, X.; Snoeck, E.; Roucau, C. *Appl. Phys. Lett.* **1994**, *65*, 1448.
- (16) Vilalta, N.; Sandiumenge, F.; Piñol, S.; Obradors, X. *J. Mater. Res.* **1997**, *12*, 38–46.
- (17) Chen, S. K.; Zhou, L.; Wang, K. G.; Wu, X. Z.; Zhang, P. X.; Feng, Y. *Phys. C Supercond.* **2002**, *366*, 190–194.
- (18) Meignan, T.; Banerjee, A.; Fultz, J.; McGinn, P. J. *Phys. C Supercond.* **1997**, *281*, 109–120.
- (19) McGinn, P.; Meignan, T.; Yeung, S.; Banerjee, A. *Appl. Supercond.* **1996**, *04*, 563–575.
- (20) Delamare, M. P.; Monot, I.; Wang, J.; Provost, J.; Desgardin, G. *Supercond. Sci. Technol.* **1996**, *9*, 534.
- (21) Yeung, S.; Banerjee, A.; Fultz, J.; McGinn, P. J. *Mater. Sci. Eng., B* **1998**, *53*, 91–94.
- (22) Daeumling, M.; Seuntjens, J. M.; Larbalestier, D. C. *Nature* **1990**, *346*, 332–335.
- (23) Zhai, W.; Shi, Y. H.; Durrell, J. H.; Dennis, A. R.; Rutter, N. A.; Troughton, S. C.; Speller, S. C.; Cardwell, D. A. *Supercond. Sci. Technol.* **2013**, *26*, 125021.
- (24) Chen, D.-X.; Goldfarb, R. B. *J. Appl. Phys.* **1989**, *66*, 2489.
- (25) Yeung, S.; Banerjee, A.; Fultz, J.; McGinn, P. J. *Mater. Sci. Eng., B* **1998**, *53*, 91–94.
- (26) Daeumling, M.; Seuntjens, J. M.; Larbalestier, D. C. *Nature* **1990**, *346*, 332–335.
- (27) Sawamura, M.; Morita, M. *Phys. C Supercond.* **2001**, *357–360*, 892–895.